Published in final edited form as:
Magn Reson Med. 2010 September ; 64(3): 672–679. doi:10.1002/mrm.22448.

Prospective Motion Correction for Single-Voxel ^{1}H MR Spectroscopy

Brian Keating[1], **Weiran Deng**[1], **J. Cooper Roddey**[2], **Nathan White**[3], **Anders Dale**[2], **V. Andrew Stenger**[1], and **Thomas Ernst**[1]

Department of Medicine, John A. Burns School of Medicine, University of Hawaii, Honolulu, Hawaii

Department of Neurosciences, University of California, San Diego, La Jolla, California

Department of Cognitive Science, University of California, San Diego, La Jolla, California

Abstract

Head motion during ^{1}H MR spectroscopy (MRS) acquisitions may compromise the quality and reliability of *in vivo* metabolite measurements. Therefore, a 3-plane image-based motion tracking module was integrated into a single-voxel ^{1}H MRS (PRESS) sequence. A series of 3 orthogonal spiral navigator images were acquired immediately prior to the MRS water suppression module in order to estimate head motion. By applying the appropriate rotations and translations, the MRS voxel position can be updated such that it remains stationary with respect to the brain. Frequency and phase corrections were applied during post-processing to reduce line-width and restore coherent averaging. Spectra acquired during intentional head motion in 11 volunteers demonstrate reduced lipid contamination and increased spectral reproducibility when motion correction is applied.

Keywords

MR spectroscopy; brain; metabolism; motion

INTRODUCTION

Brain metabolite measurements using MR spectroscopy (MRS) generally require averaging of many acquisitions from the same spatial location to obtain acceptable signal-to-noise ratio (SNR). This results in relatively long scan times and increases the likelihood that the subject will move at some point during the scan. Such concerns are particularly acute with subjects who are uncooperative and/or unable to remain still, for instance, adults who are in pain, confused, those who have movement disorders or young children. While prior work evaluated the effects of physiological motion, such as small and imperceptible head movements due to the respiratory cycle, on *in vivo* MR spectra, the current study focuses on aperiodic, bulk head motion of substantial amplitude. Such motion can cause errors and artifacts that may not be evident in typical quality assurance procedures. Even if movement is noticed by the scanner operator, subject motion is often the cause of repeated scans, resulting in inefficient use of scanner time.

*Corresponding Author: Brian Keating, Ph.D., UH-QMC Magnetic Resonance Research Center, University of Hawaii John A. Burns School of Medicine Department of Medicine, 1356 Lusitana Street, 7th Floor, Honolulu, HI 96813-2427, USA, Tel: (+1) 808-585-5158, Fax: (+1) 808-585-5160, brianrk@hawaii.edu.

Head motion compromises spectral quality in a variety of ways. First, in both stimulated echo acquisition mode (STEAM) (1) and point resolved spectroscopy (PRESS) (2) sequences, strong spoiler gradients are applied between the RF pulses to suppress unwanted coherences from outside the voxel. As a result, subject motion can introduce unpredictable phase accumulations, which result in incoherent signal averaging and can degrade the SNR of the final spectrum. Second, motion can induce changes in the magnetic field (B_0) homogeneity, which may lead to increased spectral line-width, poor water suppression, and baseline distortions. Third, since the voxel is stationary in scanner coordinates, patient movements cause the signal to be acquired from a different part of the brain than intended. If a voxel is placed in close proximity to the skull, motion can introduce lipid contamination, which, in severe cases, will dominate the spectrum. Fortunately, this type of artifact is relatively easy to detect by visual inspection of the spectra. However, since spectra from different brain regions, such as gray matter and white matter, may differ relatively subtly, errors resulting from small movements may be difficult or impossible to detect during quality assurance, resulting in inaccurate metabolite concentrations or ratios.

Previous work has focused mainly on correction of phase and/or frequency variations arising from head motion, using residual under-suppressed water peaks (3) or dedicated navigator echoes (4,5) to restore phase coherence between averages, or to discard motion-corrupted acquisitions. Such methods can improve line width and SNR of the spectra, and help with quality assurance. However, discarding acquisitions reduces SNR, sometimes unacceptably, and under-suppressing the water signal can result in distorted baselines. Critically, none of these techniques uses motion correction; therefore, it cannot be ensured that the voxel remains in the correct brain region in the presence of motion. In MRI, motion correction commonly involves use of gradient waveforms that oversample the center of k-space, and then performing motion correction during post-processing (e.g., PROPELLER (6)). Alternately, prospective motion correction schemes have been proposed that use k-space based navigators to track motion and then adapt scan planes in real-time such that they are stationary relative to the moving brain (7,8).

We have integrated a three-dimensional (3D), image-based adaptive motion correction module (PROMO) (9,10) into an ^{1}H PRESS sequence, and combined it with a novel method of water suppression cycling (11). These modifications make it possible to keep the MRS voxel fixed relative to the moving brain and perform shot-to-shot frequency and phase corrections. This approach makes it possible to obtain high-quality spectra, with accurate brain metabolite measurements, even in the presence of large head movements.

METHODS

MR methods

Figure 1 depicts a flow chart illustrating the operation of the adaptive motion correction system. The complete MRS sequence with adaptive motion correction consists of two separate modules: 1) a time-critical spiral navigator sequence that provides input to a motion estimation module, and 2) a standard PRESS sequence for localized MRS. Spectroscopy or navigator raw data are flagged to indicate whether it should be processed using the MRS reconstruction pipeline, or the spiral reconstruction/motion estimation pipeline. The latter is performed in real-time, and motion estimation data are sent back to the MRS sequence to dynamically adjust scan planes and positions such that the MRS voxel remains at a fixed position relative to the moving brain. The details of this system are described below.

The spectroscopy module is based on a short echo-time (TE) PRESS sequence (2) (TE/TR=30/3000 ms, BW=1.2 kHz, 4 dummy scans, 32 averages, 20×20×20mm voxel) with optimized slice orientations (12). The standard Siemens sequence was modified to allow

dynamic updates of slice orientations and slice positions during each repetition period, in order to maintain the voxel position stationary relative to the moving brain.

Prior to each PRESS excitation pulse, a water suppression module is played out. Weak water suppression is achieved via 4 frequency selective pulses (bandwidth 80Hz), followed by crusher gradients. A novel water suppression cycle is employed which allows shot-to-shot frequency and phase corrections using the weakly-suppressed water signal, while minimizing the residual water signal after final summation (11). Specifically, the water is under-suppressed on even acquisitions and over-suppressed on odd acquisitions, so that the water peaks naturally cancel during final signal summation, thereby avoiding the baseline distortions typically associated with weakly-suppressed residual water signal. This entire water cycling module takes 212ms.

Immediately prior to the water suppression module, a series of five spiral navigator sets are acquired to estimate the head position. Each navigator set consists of three orthogonal (sagittal, coronal, axial), low-flip angle, low-resolution, single-shot spiral images with the following parameters: flip angle 5°, TE 1.8ms, spiral-out trajectory, field of view 260mm, 32×32 nominal resolution, and slice thickness 5mm. The spiral readouts are slew rate-limited and uniformly sampled, using the trajectory of (13). Images are reconstructed using standard regridding techniques (14) and zero-padded to a resolution of 128×128. The pulse sequence for a single navigator set is shown in Fig. 2c.

Real-time image reconstruction and motion estimation is critical for the proper functioning of the adaptive motion correction scheme. If motion data feedback is not received in time, not only is the motion estimation lagging by 1 TR period, but substantial oscillations in the motion parameters develop, leading to incorrect tracking. In the interest of reducing the total navigator time, fat suppression was neglected and a minimal TE was employed. The slice excitations within a single navigator set are separated by 17ms (to allow for the spiral readout); therefore, one navigator set, consisting of 3 slices, takes approximately 50ms. Following each set of navigator slices, pre-calculation of sequence events (e.g., gradient- and rf-waveforms) is paused for 200ms to perform reconstruction of navigator images and motion estimation. Thus, since 5 navigator sets are played out, the entire navigator and motion estimation module takes approximately 1500ms, allowing it to fit into the otherwise unused “dead-time” period of each repetition (which were played out at a fixed interval of 3 seconds).

The spiral navigators use a small flip angle to ensure that the excitation of the navigator slices do not affect metabolite magnetization. In the worst case scenario, the MRS voxel is located at the intersection of all three navigator slices. Assuming a metabolite T1 of 1500ms, this would result in a signal loss of 2.2% due to incomplete T1 relaxation between the navigator excitations and the PRESS excitation (taking into account that the navigator slices are much thinner than the MRS voxel slices). However, since the navigator slices are initially centered on the magnet isocenter, this scenario is unlikely to take place. In a more typical configuration, where only one of the navigator planes intersects the voxel, the metabolite signal loss due to navigator interference is 0.33%, and therefore negligible.

Prior to each MRS scan, the magnetic field homogeneity is optimized over the voxel of interest. However, this voxel-based shim generally results in a poor shim across the brain and for the navigator acquisitions, leading to geometric distortions and artifacts in the spiral images. To eliminate these artifacts, the following method was used. First, second-order shims for the MRS examination were retained from a previously acquired whole-brain structural scan. Next, the linear shims over the MRS voxel were adjusted manually, yielding typical metabolite line widths of 0.05ppm or better. The resulting shim was thus optimized

for the MRS part of the acquisition. However, this may result in a poor overall shim for the 3 orthogonal spiral navigator scans, and lead to image artifacts. Therefore, at the very beginning of the scan, a B0 field-map was reconstructed for each of the 3 orthogonal navigator slices, using two spiral images with different TE values (ΔTE=0.5ms). Linear correction terms were estimated from these field maps for each spiral slice, and corrected during image reconstruction. This made it possible to acquire high-quality spectra while minimizing distortions and artifacts in the navigator images.

Motion estimation & correction

The state of a rigid body can be characterized by six parameters: x-, y- and z-translations, and x-, y- and z-rotations. The rigid body parameters of a subject's brain are estimated based on the current navigator images using an extended Kalman filter (15), as implemented in a 3D prospective motion estimation module (PROMO) (10,16). The Kalman filter is a general predict-and-correct scheme that uses noisy measurement data (navigator images) to update the estimate of an unknown state vector (rigid body parameters). At the beginning of each scan, a single set of three navigator images is designated as a reference. Since the motion is treated as random, the predicted state vector at any given time step is set equal to predicted parameters of the previous step. Based on these predicted parameters, the acquired navigator images are interpolated back onto the reference planes, and measurement residuals are calculated. The predicted parameters are corrected using a weighted sum of the residuals. This scheme can be considered a generalization of standard least-squares image registration to incorporate a model of the dynamics. For further details, see reference (10).

It was found that the Kalman filter can take several iterations to converge on an accurate estimate for the head's rigid-body state. For instance, a large pure rotation can cause spurious changes in estimated translations. Such "crosstalk" errors can be eliminated by acquiring two to three navigators in quick succession (10). In order to use all of the available dead time in each TR period, five navigator sets (each containing 3 orthogonal slices) were acquired before each MRS acquisition, as indicated in Fig. 2b. Using a very similar approach, White, et al. (10) report steady state errors of 150-400μm for translations and 0.2–0.3° for rotations.

Non-rigid subject motion can be a significant source of tracking error in prospective motion correction. Because PROMO navigators are image-based, rather than k-space-based, it is possible to effectively eliminate from the motion correction procedure areas of the subject's body that can move non-rigidly with respect to the brain, such as the neck and jaw (see Fig. 3). Prior to the first PRESS acquisition, 18 "training" navigator sets are acquired. These training sets are automatically registered to a previously created head atlas. Kalman filter measurement covariance parameters are then adapted so that neck and jaw regions in the navigator images do not contribute to motion estimates. This masking method markedly improves tracking accuracy (16).

After image reconstruction and motion estimation are completed, the rigid body parameters are sent back to the scan sequence. Immediately prior to each PRESS module, the orientation of the MRS voxel is updated by rotating slice-select gradients, and its location is updated by shifting the center frequencies of the radio-frequency (RF) pulses used for slice selection. In this manner, the voxel maintains a constant position relative to the moving brain. Similarly, the orientations and positions of the navigator planes are updated every TR period, in order to ensure that all of the navigator images are similar to each other, and only reflect the relative motion between successive navigator acquisitions. This procedure increases tracking accuracy, but also makes the estimated motion parameters susceptible to oscillations if the feedback is not received in real-time.

Human subjects

All subjects (n=11) were adults, healthy, and provided informed consent in compliance with the Institutional Review Board. Experiments were performed on a TIM Trio 3T whole-body scanner (Siemens Medical Systems, Erlangen, Germany) with a 12 channel phased-array head coil. All MRS scans incorporated the navigator module described above and collected motion data. Scans were performed in one of two modes: *navigated* scans updated the voxel location prior to each PRESS module, and *un-navigated* scans did not update the voxel location. The voxel was initially positioned medially in the frontal lobe, and contained mostly grey matter before motion.

Subjects were placed in the head coil, and taught to perform either an approximately 5cm superior-inferior translation ("slide toward their feet") or a 20° rotation about the superior-inferior axis ("roll head to left"). For the 4 subjects performing a translation, three scans were performed: a *baseline* scan with no motion, an *un-navigated* scan with translation, and a *navigated* scan with translation. The 7 subjects performing a rotation underwent four scans: a *baseline* with no motion, a *rotated baseline* where the rotation was performed prior to the scan with no motion during the scan, an *un-navigated* scan with rotation performed during the scan starting with the voxel in the frontal gray matter, and a *navigated* scan with rotation performed during the scan (also starting with the voxel in the gray matter). The amplitude of the rotations was chosen so that after the head rotation, the (un-navigated) voxel contained primarily white matter as determined from a quick axial gradient-echo pilot scan (TE=5ms, TR=14ms, flip angle=25°), see Fig. 4, bottom row. Because changing the orientation of the head relative to the main magnetic field also changes the field homogeneity, the linear shims for the rotated baseline, navigated and un-navigated scans were optimized over the MRS voxel with the head in the rotated position.

Data and statistical analyses

Data were preprocessed using a customized Matlab program. Signals from individual channels were combined using constant weightings based on the coil sensitivities at the initial voxel position. First, individual FIDs were frequency and phase corrected using the under-suppressed or over-suppressed water signal. Final signal averaging was performed using a variable scaling factor between the over- and under-suppressed FIDs, in order to minimize the baseline distortion of the final spectrum. Metabolite levels were quantified with LCModel, using a 3T basis data set that included the resonances of N-acetyl-aspartate (NAA), creatine plus phosphocreatine (Cr), total choline (Cho), myo-inositol (mI), glutamate, glutamine, and GABA, as well as macromolecule and lipid resonances. The effects of motion correction were evaluated by calculating the percent differences in NAA, Cho, and Cr concentrations, as well as the Cho/Cr ratios, between scans with motion and the baseline scan (without motion) for each subject. Significance of differences between data acquired with and without motion was then determined using paired t-tests.

RESULTS

Figure 5 shows the motion plots and frontal grey matter spectra for a typical subject who performed a z-translation. In the navigated and un-navigated cases the estimated motion trajectories were similar, with a z-translation of approximately -30mm (un-navigated) and -42mm (navigated), relatively small x- and y-translations (<8mm), and small rotations (each <5°). In the un-navigated case, the head moved in such a way that the stationary voxel intersected the scalp, causing severe contamination of the spectrum with lipid signal (Fig. 5a). However, during the navigated scan the voxel remained stationary relative to the brain, and very little lipid signal is visible (Fig. 5b). Spectral quantification was not possible in the un-navigated scans of the subjects who performed translations.

When head movement is smaller, there may be no lipid contamination, and the effects on the spectra are more subtle. Figure 4 shows three spectra acquired from one subject who performed z-rotations (i.e., about the inferior-superior axis). The voxel positions for the navigated and un-navigated scans are overlaid on pilot gradient echo images that were obtained before and after the motion. In the baseline spectrum of Fig. 4, the Cho peak is smaller in height than the Cr peak, suggesting the voxel is predominantly located in the grey matter. (17) This pattern is reversed in the un-navigated spectrum, which shows a Cho/Cr peak height ratio greater than 1 (middle spectrum). When the same head movement is performed but adaptive motion correction is enabled, the resulting spectrum closely resembles that of the baseline condition; for instance, the original lower Cho/Cr ratio is essentially recovered (right spectrum).

These observations are confirmed in Table 1, which shows the percent changes between spectra with motion (navigated and un-navigated) and without motion (i.e., baseline) for the NAA, Cho, and Cr concentrations, as well as the Cho/Cr and NAA/Cr ratios. For each of these metabolites, the mean concentration difference between the navigated and baseline spectra is less than the difference between the un-navigated and baseline spectra. Furthermore, the variance of the relative concentration difference between navigated and baseline scans is also reduced relative to the un-navigated scans for the 3 metabolites evaluated, indicating greater reliability of spectral quantification in the navigated case. Paired t-tests (α=0.05) show that the Cho/Cr ratios from the un-navigated spectra are significantly different than those obtained at baseline (without motion), whereas the ratios of the navigated spectra are similar to those obtained at baseline. This demonstrates that the navigated sequence is better able to reproduce the original grey matter spectra of the baseline scans. The line-widths of the baseline (0.041±0.012), navigated (0.043±0.012) and un-navigated spectra (0.046±0.007) are similar and do not differ statistically; however, the SNR of the baseline spectrum (20.9±4.2) is significantly higher than that of both the navigated (18.1±4.3, p=0.04) and un-navigated (16.4±4.9, p=0.04) spectra.

Bulk head movements may affect the magnetic field distribution within the brain. Therefore, preliminary tests were conducted with water suppression turned off to characterize the effects of motion on water line-width and frequency shift. The water frequency showed an approximately linear dependence on motion parameters, whereas changes in line-width with motion were more variable, with an approximately quadratic dependence on the motion parameters. At worst, the water peak full-width at half-maximum increased by approximately 0.06 ppm for 35mm z-translations and 0.03–0.08 ppm for 30° z-rotations. The water peak frequency shifted by approximately 3×10^{-3} ppm/mm for z-translations and 2×10^{-3} ppm/deg for z-rotations.

DISCUSSION

Our study demonstrates that adaptive motion correction can reduce many of the motion-induced artifacts in single-voxel ^{1}H MRS. In situations where normal-appearing brain tissue is evaluated, the appearance of strong lipid signals (as in Fig. 5) may be noticed by a scanner operator or during visual quality assurance, and this data would be discarded or the scan would be repeated. However, many brain lesions, such as tumors or abscesses, have intrinsically high lipid concentration, so the presence of a strong lipid signals cannot be used as an indicator of head motion. Similarly, even when normal-appearing brain tissue is scanned, the head motion may be such that the voxel remains within the skull, but is nonetheless in the wrong location. In such a case, a good spectrum may be obtained, but the metabolite concentrations would not accurately reflect the content from the intended voxel location, as illustrated in Fig. 4.

Motion navigators commonly base motion estimation on frequency-domain (k-space) data. One problem inherent to such techniques is that they cannot fully account for the complex movements of the human body. In a typical brain scan, the excitation volume will include the neck, jaw, face, and skull, which can all move independently. Modeling such an assembly as a rigid body will necessarily lead to errors in the estimated motion parameters; therefore, an image-based navigator was used here. An attractive alternative is optical tracking, wherein external cameras track markers affixed to the subject's head (18,19) In addition to requiring additional equipment, the proper functioning of such a system necessitates an unobstructed line of sight between the cameras and markers, which can be awkward to achieve. However, optical tracking does not interfere with the MR measurement process, and allows very high tracking rates, in the range of 100 tracking points per second.

Image-based prospective navigators are well-suited for use in localized MRS, since such sequences typically have a substantial "dead time" between excitations to allow for recovery of longitudinal magnetization. Consequently, the navigator could be integrated with no penalty in scan time. Of note, optimization of the spiral reconstruction would make it possible to reduce the total navigator time to approximately 500ms. Since the navigator/PROMO portion of our sequence is fairly self-contained, it could be used in many MRI, MRS or spectroscopic imaging sequences with minimal changes.

The temporal resolution of any MR-based navigator is inherently limited. In our sequence, the time between the final navigator acquisition in a given TR period and the subsequent PRESS excitation is about 430ms, during which time a non-negligible amount of motion can take place. To improve the estimation of head pose at the moment of PRESS excitation, the five consecutive motion estimator sets acquired in each TR period may be used to estimate the velocity of the head's trajectory and predict the position at the time of the MRS acquisition. Additionally, FIDs acquired during a period of rapid motion can be discarded.

Since the navigator planes move with the head, navigator images only reflect relative motion since the previous update. Thus, one would expect the tracking accuracy to be lower during periods of rapid motion. The advantage of this approach is however that accuracy is unaffected by the absolute displacement of the head, even for large movements. Conversely, rapid movements with small amplitude, for instance due to involuntary tremors, may cause negligible shifts in the voxel position, and the resulting phase accumulation can be corrected using the water suppression cycling presented here. While we were able to judge the accuracy of the motion parameters by visual inspection of the navigator images, a quantitative investigation is needed to clarify the trade-off between navigator resolution, navigator SNR and accuracy of the motion parameters derived. We intend to do this by comparing the MR-based tracking data with those of the "gold-standard" of optical tracking. It is worth noting that, in contrast to many MRI applications, sub-millimeter tracking accuracy is generally not required for human spectroscopic acquisitions, which typically have voxel dimensions on the order of centimeters.

For sufficiently large motions, shifts in the center frequency can diminish the effectiveness of the water suppression. Our studies indicate that for a 20° z-rotation, one can expect a frequency shift of up to 0.04ppm, and for a 25mm z-translation the frequency typically shifts by 0.075ppm. Thus, for the water suppression pulses used in the current study (band width = 80Hz ≈ 0.6ppm), the reduction in water suppression effectiveness is negligible. However, loss of effective water suppression may become an issue if narrow-bandwidth water suppression is used in the presence of large amplitude motion.

Additionally, motion-induced changes in the B_0-distribution will reduce the quality of the voxel shim. Therefore, a linear shim update calculated from a rapidly acquired field map

would be an ideal complement to the navigator presented here, and is in fact a requirement for obtaining high-quality spectra in the presence of large head movements. Such a method of real-time dynamic shimming is being developed, but is beyond the scope of the current publication. While the appearance of transient eddy currents prevents dynamic updating of higher-order gradient shims, linear shim updates are most likely sufficient to obtain acceptable spectral line widths for most subjects and movements.

Yet another consequence of motion on MRS acquisitions when using multi-channel coils is the effect of changes in the voxel position on the phase and amplitude of the signal received by each coil. Phase changes are continuously corrected by the water suppression cycling presented here, in the same way as motion-induced phase changes. However, magnitude changes caused by large shifts in position may lead to sub-optimal coil combinations, and a possible reduction in SNR. For the range of motions investigated in this study, any such reduction in SNR was likely small compared to the detrimental effects of poor shim; however, the residual water signal in each spectrum could be used to recalculate coil weightings from shot to shot and thereby ensure optimal signal-averaging.

Our results indicate that the addition of an image-based navigator to an MRS sequence is a viable method for increasing spectral quality for reliable brain metabolite measurements. Since localized MRS examinations typically involve relatively large dead-times between individual acquisitions, adaptive motion correction can be implemented with little or no penalty in scan time. Therefore, we predict that adaptive motion correction will eventually become standard for localized ^{1}H MRS studies of the brain, and possibly also for spectroscopic imaging (SI) studies. However, our method needs to be validated in a larger study which includes non-compliant subjects.

Acknowledgments

This project was supported by NIH grants 1R01 DA021146 (TE), U54 56883 (SNRP), K02-DA16991, and G12 RR003061-21 (RCMI). We would like to thank Drs. Steven Buchthal and Linda Chang for valuable feedback and support of this work.

References

1. Frahm JMH, Haenicke W. Localized high-resolution proton NMR spectroscopy using stimulated echoes: initial applications to human brain in vivo. J Magn Reson. 1987; 72:502–508.
2. Bottomley PA. Spatial localization in NMR spectroscopy in vivo. Ann N Y Acad Sci. 1987; 508:333–348. [PubMed: 3326459]
3. Star-Lack, JM.; Adalsteinsson, E.; Gold, GE.; Spielman, DM. ISMRM. Sydney, Australia: 1998. Motion correction and lipid suppression for in vivo 1H MRS — applications to the study of the human kidney and liver; p. 1472
4. Bhattacharyya PK, Lowe MJ, Phillips MD. Spectral quality control in motion-corrupted single-voxel J-difference editing scans: An interleaved navigator approach. Magn Reson Med. 2007; 58(4): 808–812. [PubMed: 17899594]
5. Thiel T, Czisch M, Elbel GK, Hennig J. Phase coherent averaging in magnetic resonance spectroscopy using interleaved navigator scans: Compensation of motion artifacts and magnetic field instabilities. Magn Reson Med. 2002; 47(6):1077–1082. [PubMed: 12111954]
6. Pipe JG. Motion correction with PROPELLER MRI: Application to head motion and free-breathing cardiac imaging. Magn Reson Med. 1999; 42(5):963–969. [PubMed: 10542356]
7. Ward HA, Riederer SJ, Grimm RC, Ehman RL, Felmlee JP Jr. CRJ. Prospective multiaxial motion correction for fMRI. Magn Reson Med. 2000; 43(3):459–469. [PubMed: 10725890]
8. André JW, van der Kouwe TB, Dale Anders M. Real-time rigid body motion correction and shimming using cloverleaf navigators. Magn Reson Med. 2006; 56(5):1019–1032. [PubMed: 17029223]

9. Shankaranarayanan, A.; Roddey, JC.; White, N.; Han, ET.; Rettmann, D.; Santos, J.; Schmidt, E.; Dale, A. ISMRM. Berlin, Germany: 2007. Motion insensitive 3D imaging using a novel real-time image-based 3D PROspective MOtion correction method (3D PROMO).
10. Nathan White CR, Shankaranarayanan A, Han E, Rettmann D, Santos J, Kuperman J, Dale A. PROMO - Real-time Prospective Motion Correction in MRI Using Image-based Tracking. Magn Reson Med. 2010; 63(1):91–105. [PubMed: 20027635]
11. Ernst, T.; Jikun, L. ISMRM. Honolulu, HI, USA: 2009. Phase Navigators for Localized MR Spectroscopy Using Water Suppression Cycling.
12. Ernst T, Chang L. Elimination of artifacts in short echo time 1H MR spectroscopy of the frontal lobe. Magn Reson Med. 1996; 36(3):462–468. [PubMed: 8875419]
13. Cline HE, Zong X, Gai N. Design of a logarithmic *k*-space spiral trajectory. Magn Reson Med. 2001; 46(6):1130–1135. [PubMed: 11746579]
14. Jackson JMC, Nishimura D, Macovski A. Selection of a convolution function for Fourier inversion using gridding. IEEE Trans Med Imaging. 1991; MI-10(3):473–478. [PubMed: 18222850]
15. Anderson, JB. Optimal Filtering: Prentice-Hall. 1979.
16. Roddey, JC.; Shankaranarayanan, A.; Han, E.; White, N.; Kuperman, J.; Dale, A. ISMRM. Toronto, Ontario, Canada: 2008. Motion insensitive imaging using 3D prospective motion (PROMO) correction with region-of interest tracking.
17. Schuff N, Ezekiel F, Gamst AC, Amend DL, Capizzano AA, Maudsley AA, Weiner MW. Region and tissue differences of metabolites in normally aged brain using multislice 1H magnetic resonance spectroscopic imaging. Magn Reson Med. 2001; 45(5):899–907. [PubMed: 11323817]
18. Zaitsev M, Sakas G, Hennig J, Speck O. Magnetic resonance imaging of freely moving objects: prospective real-time motion correction using an external optical motion tracking system. Neuroimage. 2006; 31(3):1038–1050. [PubMed: 16600642]
19. Eviatar, HSB.; Sharp, JC.; Rendell, J.; Alexander, ME. ISMRM. Philadelphia, PA, USA: 1999. Real time head motion correction for functional MRI.

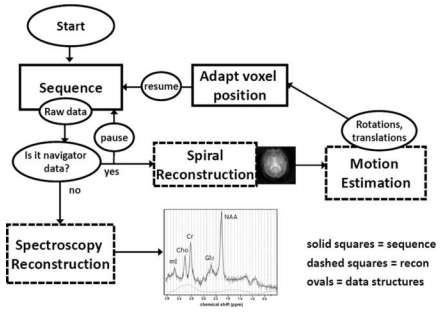

FIG. 1.

The navigated sequence pipeline. Solid squares represent sequence calculations, dashed boxes are reconstruction computations and ovals represent data structures. It is necessary to explicitly pause the sequence pre-calculation before the PRESS excitation to ensure the sequence does not calculate the gradient and RF waveforms before updated motion data are available.

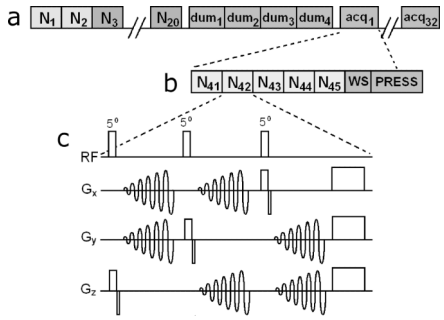

FIG. 2.

(**a**) Diagram of the complete navigated PRESS sequence. (**b**) A zoomed in view, depicting the navigators in one PRESS acquisition. Both dummy and actual acquisitions are preceded by five spiral navigators. (**c**) The gradient and rf waveforms for a single three-slice navigator. Each “N” here refers to the entire module depicted in (**c**), plus a 200ms pause for reconstruction, motion estimation and feedback. N1 and N2 are used to create field maps, N3–N20 project brain masks on the navigator planes (Fig. 2) and subsequent navigators track the head motion.

FIG. 3.
Typical navigator images with brain masks overlaid in yellow. Coronal (left) axial (center) and sagittal (right) slices.

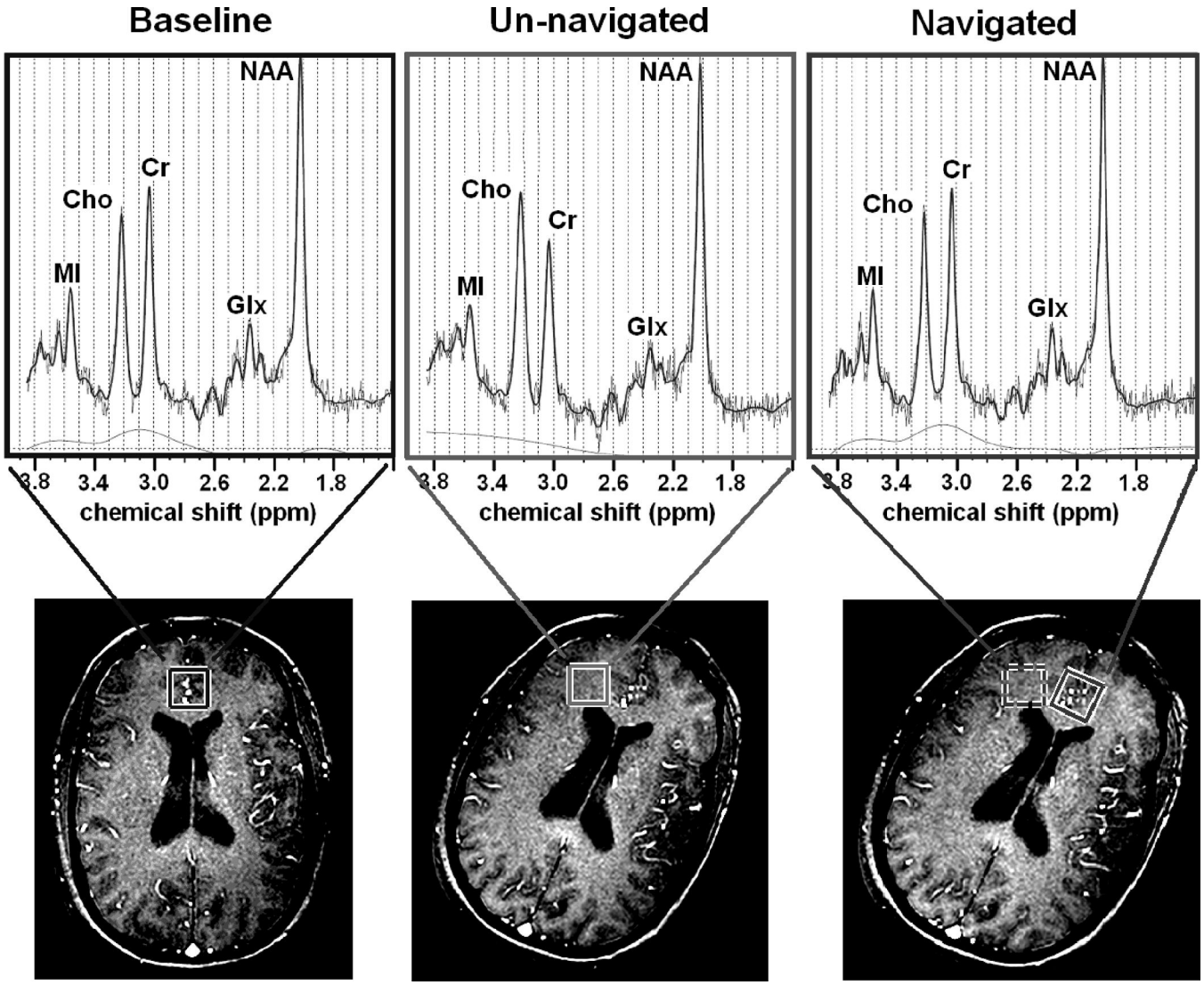

FIG. 4.

Top row: spectra acquired from baseline (left), un-navigated (center) and navigated (right) scans. Bottom row: pilot gradient echo images taken immediately after each scan. All scans started with the head in the baseline orientation (bottom left). In the baseline scan, no motion was performed. In the navigated and un-navigated cases, the motion was similar: a 21° (un-navigated) or 25° (navigated) z-rotation. Translations and other rotations were small. For all scans, the voxel was initially placed in the medial frontal grey matter and subjects were instructed perform the rotation early in the scan -- most of the acquisitions for the navigated and un-navigated spectra were acquired after the motion was performed.

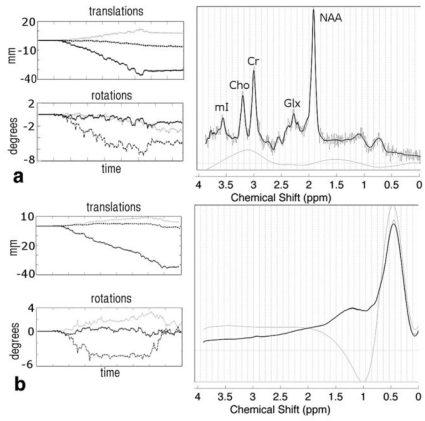

FIG. 5.

Motion plots and spectra for the navigated and un-navigated scans in one subject who performed a –z translation. In the motion plots, dashed lines refers to x-, grays lines to y- and black lines to z-rotations and translations. In the un-navigated case (**a)**, the lipid signal dominates the spectrum, making quantification of metabolite concentrations impossible. In the navigated case (**b**), the voxel remains away from the skull, and a useable spectrum is obtained.

Table 1

Percent difference and standard deviation in NAA, Cho, Cr concentrations and the Cho/Cr ratio between scans with motion and the baseline scan without motion. The p-value lists the result of a paired t-test between the two conditions.

	un-navigated – baseline (% baseline)	**navigated – baseline (% baseline)**
NAA	−6.5 ± 17.4 (p=0.329)	−3.2 ± 10.1 (p=0.410)
Cho	10.5 ± 30.7 (p=0.455)	−8.6 ± 10.1 (p=0.140)
Cr	−12.7 ± 20.8 (p=0.110)	−6.2 ± 14.5 (p=0.225)
Cho/Cr	26.6 ± 21.4 (**p=0.035**)	−2.4 ± 9.4 (p=0.565)
NAA/Cr	8.6 ± 11.3 (p=0.142)	4.4 ± 11.2 (p=0.468)